FPASMR: AN L\X-BAND FULL POLARIZATION APERTURE SYNTHESIS MICROWAVE RADIOMETER

Yinan Li, Hao Li, Rongchuan Lv, Bing Li, Yanming Li, Shangyu Shen, Dizhu Wang

Xian Institute of Space Radio Technology, Xian 710100, China

ABSTRACT

L\X-band Full Polarization Aperture Synthesis Microwave Radiometer (FPASMR) is a 2-D aperture synthesis radiometer working at L and X-band with full polarization measurement for obtaining high precise measurement of sea salinity and soil moisture. FPASMR consists of dual Y-shaped arrays containing 23 L-band antennas per arm plus one in the center in L-band array and the same numbers of X-band antennas in X-band array. Some early demonstration results of antenna, optical module and calibration are also present.

***Index Terms*—**full polarization, aperture synthesis microwave radiometer, sea salinity, soil moisture.

1. INTRODUCTION

Sea salinity and soil moisture are closely related to the world climate and the water cycle. Previous studies have shown that sea salinity and soil moisture can be measured by using L-band microwave radiometer [1, 2]. However, it is difficult for the L-band real aperture antenna to obtain high space resolution in satellite application because of its large size and weight.

As a new array interferometric microwave radiometric imaging system, aperture synthesis microwave radiometer [3] forms a large physical observation aperture by a thinned array of single small-aperture antennas. This can reduce the antenna size and weight, and can be placed in different spatial locations to observe the target for interferometry, which makes it easier for satellite application. Then, in order to obtain the brightness of the target temperature, which consists of physical information of the radiator radiate medium, Fourier transformation to the result of the interferometer is accomplished. At the same spatial resolution, compared with real aperture radiometers, in which brightness temperature (TB) maps are obtained by mechanical scan through a large antenna, aperture synthesis radiometers reduce the collect area of real antenna and obtain the TB image through Fourier synthesis on a snapshot basis.

However, |in order to obtaining high precision of sea salinity and soil moisture, X-band full polarization radiometry [2] which can provide surface temperature, roughness, precipitation for sea and land observation provides auxiliary measurements for L-band radiometry. Thus, the measurement precision will be improved.

2. SYSTEM DESCRIPTION

L\X-band Full Polarization Aperture Synthesis Microwave Radiometer (FPASMR) is working at L and X-band with full polarization measurement. Its dual Y-shaped arrays containing 23 L-band antennas per arm plus one in the center in L-band array and the same numbers of X-band. Due to the diameter of the L-band array (>8m), it is necessary to fold the L-band arms to fit into the available launcher volume but not necessary for X-band array which is small enough. The system contains four segments which is L-band subsystem, X-band subsystem, calibration subsystem (CAS) and power distribution and control unit (PDCU). Specification of FPASMR is shown in Tab. 1. The model of FPASMR is shown in Fig. 1.

Tab. 1 Specification of FPASMR

Parameter	FPASMR	
	L-band	X-band
Center frequency	1.415GHz	10.7GHz
Bandwidth	20MHz	100MHz
Minimum spacing	0.88λ	1λ
Integration time	1s	1s
Space resolution (@800Km orbit)	30~100km	20~60km
FOV (@800Km orbit)	>1000km	>1000km
Snap-shot sensitivity	1.6~3.8K	1~2.2K
Topology of the LO	Single LO	Centralized reference clock and internal LO in each receiver
Amount of antennas	70	70
Antenna array	Y	
Polarization	V, H, 3, 4	
Quantization	10-bits for power measurement 1-bit for correlation	
IQ	Digital IQ	
Power measurement	Digital power measurement	
Frequency response	Digital filter	

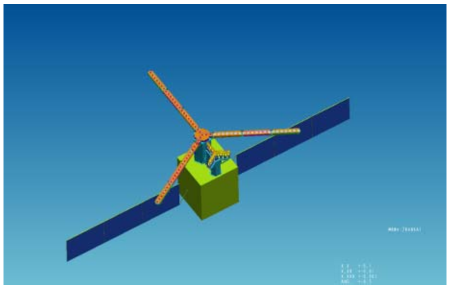

Fig. 1 The model of FPASMR

2.1 L-BAND SUBSYSTEM

L-band subsystem contains 70 L-band pre-receivers (LPR) and an integrative L-band central receiver and digital correlation unit (LRCU).

2.1.1 LPR

An LPR (Fig. 2) consists of an L-band microstrip antenna with dual polarization, two L-band low noise amplifiers to pre-amplify the V and H polarization signal from the antenna and a dual L-band channel optical transmitter which consists of a high speed DFB laser, impedance matching circuit and driving circuit. The RF signal is modulated to optic by optical transmitter (Fig. 3) and transmitted to LRCU by optical fibers. Because of about 30dB insertion loss, the input signal must be amplified about 50dB by the LNAs to ensure the sensitivity of the system.

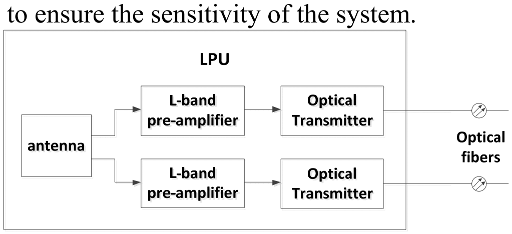

Fig. 2 The block diagram (Upper) and photograph (lower) of LPR

Fig. 3 The optical transmitter (upper) and optical receiver (lower)

2.1.2 LRCU

The LRCU (Fig. 4) consist of 140 optical receivers and 140 center receivers. A single LO distributes to all 140 channels and the digital correlator. All of the units are assembled in one structure and connected with each other by SMP connectors. The optic signal is received and is transmitted to RF signal by optical receivers which consist of high speed photodetectors and broadband amplifiers. Then, after passing by band pass filters, mixer, low pass filters, IF amplifiers in center receivers, the IF output will be obtained. Lastly, after AD sampling, digital power measurement, digital filter and correlation in the digital correlator, all of the visibility functions and power measurements can be obtained. This receiving topology can not only reduce the complexity of arms and LO structure, but also ensure the phase and amplitude of each receiving channel.

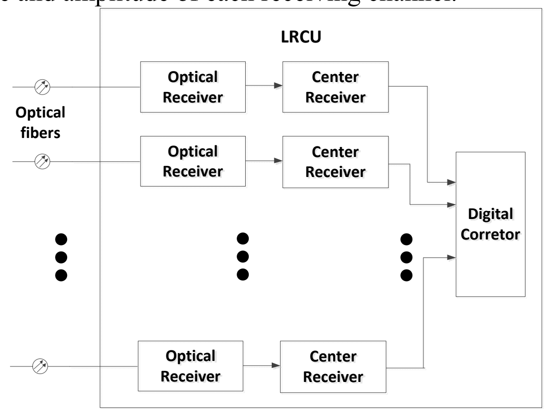

Fig. 4 The block diagram of LRCU

2.2. X-BAND SUBSYSTEM

A block diagram of X-band subsystem is shown in Fig. 5. X-band subsystem contains 70 X-band front-end receivers (XFER) and an X-band digital correlation unit (XDCU).

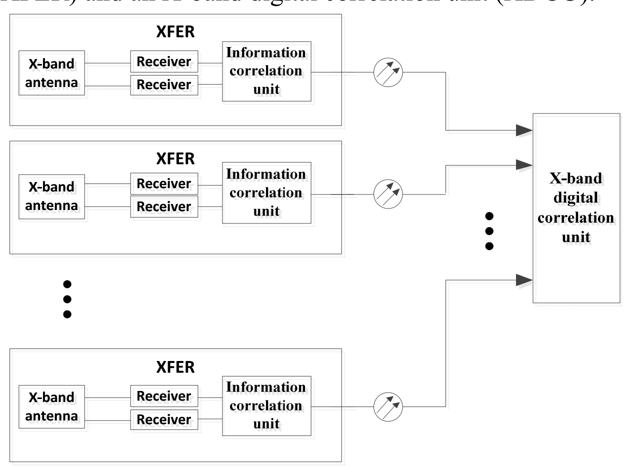

Fig. 5 The block diagram of X-band subsystem

Different to the L-band receiving topology, One XFER which has the same receiving topology with SA-PAU [3] consists of an X-band dual polarization horn antenna, a dual polarization front-end single-band receiver and an X-band information correlation unit. The output signals of the two receiving channels are digitalized by the information correlation unit. Digital filtering, 10-bits digital power measurement and 1-bit cutting processing are also carried out by the information correlation unit. Due to the 1-bit cutting processing, the data transmission and processing

capability of correlation in XDCU will be reduced. Consequently, the systematic complexity will be reduced.
The output digital signal of XFER is transmitted to XDCU through optical fibers, and after the digital data processing which is similar to L-band, all of the visibility functions can be obtained in XDCU.

2.3. Calibration

The calibration of the system is very important. Because of the large antenna array and dual Y-shaped structure, the traditional end to end calibration is difficult to carry out. Now, two calibration methods are considered. The first one is the noise injection method (CAS) which has been applied in SMOS [4] and the second one is the array rotation method [5]. Comparing to the noise injection method used in SMOS, the array rotation method can greatly reduce the system complexity, though, the new method must be verified in ground and in flight in the future. In FPASMR, both the noise injection method and the array rotation method are carried out.
The noise injection radiometer (NIR) is used to fulfill absolute calibration. The structure of NIR is similar to NIR of MIRAS [6].

2.4. PDCU

The PDCU consists of several arm PDCUs and a central PDCU. L-band Arm PDCUs provide secondary power to every LPR, send commands (TC) to LPR and receive TMs from LPR. X-band arm PDCUs provide secondary power to every XFER, send TCs to XFER and receive TMs from XFER.
The central PDCU supplies power to all L-band and X-band arm PDCUs which are the terminal of the central PDCU, send TCs to arm PDCUs, receive TMs from arm XFERs and receive remote sensing data from LRCU and XDCU. Then, all of the data will be packed and sent to the satellite.

3. DEMONSTRATION EXPERIMENT

3.1. Antenna demonstration experiment

A demonstration antenna which has seven units of L-band and X-band antennas and Y-shaped structures were produced to demonstrate the performance of the array. The demonstration experiment was carried out in anechoic chamber where antenna patterns were obtained (Fig. 6, Fig. 7).

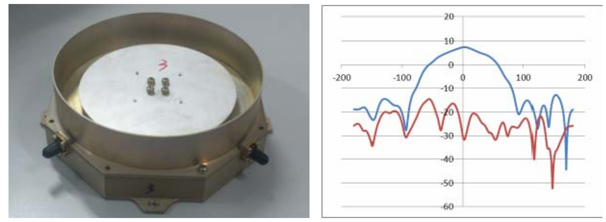

Fig. 6 The photograph of demonstration L-band antenna (left) and antenna patterns (right)

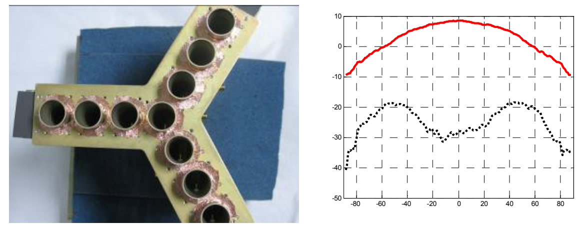

Fig. 7 The photograph of demonstration X-band antenna (left) and antenna patterns (right)

3.2. Performance of optical transmission

The RF signal transmission by optical module which consists of an optical transmitter, optical fibers and an optical receiver is first used in radiometric. Therefore the performance of optical transmission is very important and the demonstration experiment was carried out. The experiment consists of stability of delay, insertion loss, group delay, phase noise and linearity.
The stability of delay, insertion loss, group delay and phase noise of optical module is tested with the relevant instruments and the result is shown in Tab. 2.

Tab. 2 Result of experiment.

Parameter	Result
Stability of delay	0.0007ns/℃
Insertion loss	28.5dB
Group delay	0.017ns
Phase noise	-110.9dBc@10Hz -121.1dBc@100Hz -130.7dBc@1kHz

Linearity experiment using the same structure of L-band subsystem results in a Linearity of 0.9999 which is the same with that without an optical module (Fig. 7 and Fig. 8). Therefore, the optical module will not affect the linearity of the transmission channel.

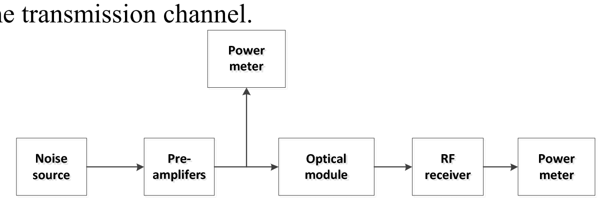

Fig. 7 The experimental setup.

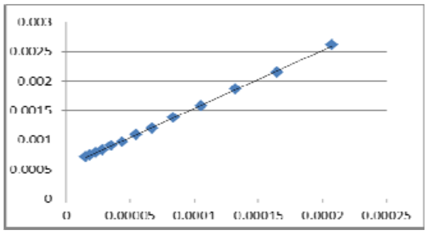

Fig. 8 Result of linearity

3.3. Calibration experiment

The two-level noise injection method and U-noise injection method [7] was carried out. The experimental setup is shown in Fig. 9 consisting of the noise source, L-band demonstration receivers, optical modules and an information collection instrument which can collect the IF signal from receivers and can fulfill processing programs.
Firstly, a two-level noise about 75K and 800K (C-noise) obtained by changing the attenuator is injected into two parallel receivers and G (FWF at origin) is obtained. Secondly, U-noise is injected into the receivers and the offsets of visibility can be obtained. The S parameter of the noise injection circuit can be measured by VNA. The results of the two-level noise injection method and the U-noise injection method are shown in Fig. 10.

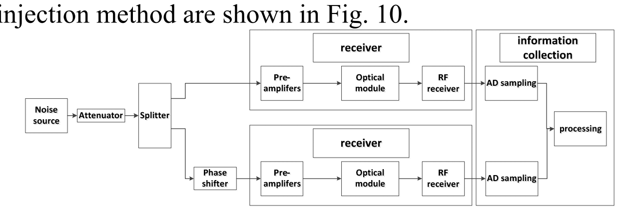

Fig. 9 Calibration experimental setup

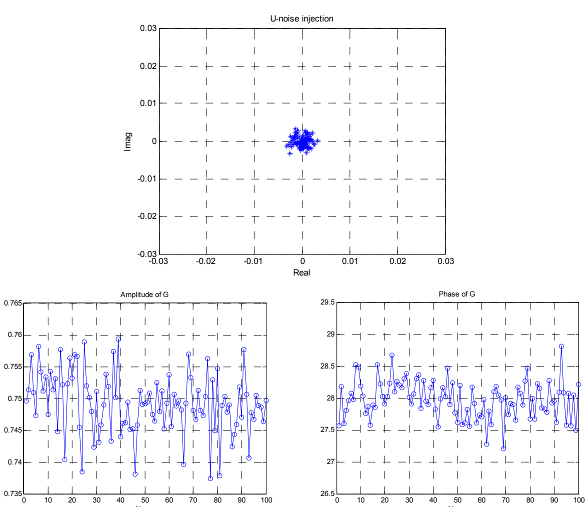

Fig. 10 Results of U-noise injection method (upper) and two-level noise injection method (lower)

The Change of the phase shifter will cause the change of the phase of input of one receiver, and the different phase of visibility can be obtained as a result. Using the G, the calibration phase will be obtained. The calibration accuracy is shown in Fig.11 and the errors Std. is about 0.16°.

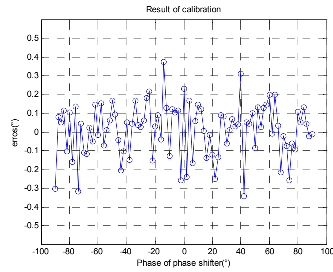

Fig. 11 Result of calibration accuracy

4. SUMMARY

Auxiliary data for sea salinity and soil moisture measurement can be acquired by FPASMR with an X-band full polarization radiometry. Consequently, the measurement accuracy can be improved. The system consisting of an antenna unit and an optical module has been demonstrated and the calibration method has been carried out and verified. Now, FPASMR is in development and the new calibration method is under investigation.

5. REFERENCES

[1] D. M. Le Vine, "ESTAR：A synthetic aperture microwave radiometer for remote sensing applications", Proc IEEE, 82:1787-1801, 1994.
[2] Peter W. Gaiser, Karen M. St, et al, "The WindSat spaceborne Polarimetric microwave radiometer: sensor description and early orbit performance," IEEE Trans. Geosci. Remote Sens., vol.42, No.5: 2347-2361, 2004.
[3] I. Ramos-Perez, A. Camps, et al, "Synthetic Aperture PAU: a New Instrument to Test Potential Improvements for Future SMOSops", Proceedings of the IGARSS 2007, pp. 247-250.
[4] I. Corbella, F. Torres, et al, "MIRAS End-to-End Calibration: Application to SMOS L1 Processor", IEEE Trans. Geosci. Remote Sens., vol. 43, No. 5, May 2005.
[5] Rong Jin, Qingxia Li, et al, "An On-Board External Calibration Method for Aperture Synthesis Radiometer by Rotation", IEEE Trans. Geosci. Remote Sens. Letters, vol. 9, No. 5, September 2012.
[6] Andreas Colliander, Lasse Ruokokoski, et al, "Development and Calibration of SMOS Reference Radiometer", IEEE Trans. Geosci. Remote Sens., vol. 45, No. 7, July 2007.
[7] Ignasi Corbella, et al, "MIRAS End-to-End Calibration: Application to SMOS L1 Processor", IEEE Trans. Geosci. Remote Sens., vol. 43, No. 5, May 2005.